



# D2.1: Product Validation and Algorithm Selection Report (PVASR) and D2.4: Algorithm Development Plan (ADP)

Reference: CCI-LAKES-0026-PVASR-ADP

Issue: 1.1

Date: Apr. 24, 2020



Chronology Issues:			
Issue:	Date:	Reason for change:	Author
1.0	19 Mar 2020	Initial Version	S. Simis et al.
1.1	24 Apr. 2020	Revision following ESA review	S. Simis et al.

People involved in this issue:			Signature
Authors:	Stefan Simis, Xiaohan Liu	Plymouth Laboratory	Marine
	Jean-François Crétau	LEGOS	
	Hervé Yésou	SERTIT	
	Erik Malnes, Hannah Vickers	NORCE	
	Pablo Blanco	TRE Altamira	
	Chris Merchant, Laura Carrea	University of Reading	
	Claude Duguay	H2O Geomatics	
Internal review:	Stefan Simis	Plymouth Laboratory	Marine
Approved by:	B. Coulon	CLS	
Authorized by:	C. Albergel	ESA	

Distribution:		
Company	Names	Contact details
ESA	A.M. Trofaier C. Albergel P. Cipollini	<a href="mailto:Anna.Maria.Trofaier@esa.int">Anna.Maria.Trofaier@esa.int</a> <a href="mailto:Clement.Albergel@esa.int">Clement.Albergel@esa.int</a> Paolo.Cipollini@esa.int
BC	K. Stelzer	<a href="mailto:kerstin.stelzer@brockmann-consult.de">kerstin.stelzer@brockmann-consult.de</a>
CLS	B. Coulon B. Calmettes	<a href="mailto:bcoulon@groupcls.com">bcoulon@groupcls.com</a> <a href="mailto:bcalmettes@groupcls.com">bcalmettes@groupcls.com</a>
CNR	C. Giardino	<a href="mailto:ggiardino.c@irea.cnr.it">ggiardino.c@irea.cnr.it</a>
GeoEcoMar	A. Scrieciu	<a href="mailto:albert.scrieciu@geoecomar.ro">albert.scrieciu@geoecomar.ro</a>

Distribution:		
Company	Names	Contact details
H2OG	C. Duguay	<a href="mailto:claude.duguay@h2ogeomatics.com">claude.duguay@h2ogeomatics.com</a>
LEGOS	J.F. Créteaux	<a href="mailto:jean-francois.creteaux@legos.obs-mip.fr">jean-francois.creteaux@legos.obs-mip.fr</a>
NORCE	E. Malnes	<a href="mailto:eima@norceresearch.no">eima@norceresearch.no</a>
PML	S. Simis	<a href="mailto:stsi@pml.ac.uk">stsi@pml.ac.uk</a>
SERTIT	H. Yésou	<a href="mailto:herve.yesou@unsitra.fr">herve.yesou@unsitra.fr</a>
TRE-ALTAMIRA	P. Blanco	<a href="mailto:pablo.blanco@tre-altamira.com">pablo.blanco@tre-altamira.com</a>
UoR	C. Merchant L. Carrea	<a href="mailto:c.j.merchant@reading.ac.uk">c.j.merchant@reading.ac.uk</a> <a href="mailto:l.carrea@reading.ac.uk">l.carrea@reading.ac.uk</a>
UoS	A. Tyler E. Spyrakos	<a href="mailto:a.n.tyler@stir.ac.uk">a.n.tyler@stir.ac.uk</a> <a href="mailto:evangelos.spyrakos@stir.ac.uk">evangelos.spyrakos@stir.ac.uk</a>

## Table of Contents

<b>1. Introduction</b> .....	<b>5</b>
<b>2. Lake Water Level (LWL) algorithms</b> .....	<b>5</b>
2.1. Candidate algorithms for LWL .....	5
2.2. Validation results for LWL .....	6
2.3. Identified issues for LWL .....	6
2.4. Future improvements for LWL .....	6
2.5. LWL References .....	7
<b>3. Lake Water Extent (LWE) algorithms</b> .....	<b>8</b>
<b>3.1. LWE-optical approach</b> .....	<b>8</b>
3.1.1. Candidate algorithms for the LWE-optical approach .....	8
3.1.2. Existing validation results for the LWE-optical approach .....	8
3.1.3. Identified issues for the LWE-optical approach .....	9
3.1.4. Future improvements for the LWE-optical approach .....	10
3.1.5. LWE-optical references .....	10
<b>3.2. LWE-SAR approach</b> .....	<b>11</b>
3.2.1. Candidate algorithms for the LWE-SAR approach .....	11
3.2.2. Existing validation results for the LWE-SAR approach .....	12
3.2.3. Identified issues for the LWE-SAR approach .....	12
3.2.4. Future improvements for the LWE-SAR approach .....	13
3.2.5. LWE-SAR references .....	13
<b>4. Lake Surface Water Temperature (LSWT) algorithms</b> .....	<b>14</b>

4.1. Candidate algorithms for LSWT .....	14
4.2. Existing validation results for LSWT.....	14
4.3. Identified issues for LSWT.....	14
4.4. Future improvements for LSWT.....	15
4.5. LSWT References .....	16
5. Lake Ice Cover (LIC) algorithms.....	16
5.1. Candidate algorithms for LIC .....	16
5.2. Validation results for LIC .....	16
5.3. Identified issues for LIC.....	18
5.4. Future improvements for LIC.....	19
5.5. LIC References.....	19
6. Lake Water Leaving Reflectance (LWLR) algorithms.....	19
6.1. Candidate algorithms for LWLR .....	19
6.2. Validation results for LWLR.....	23
6.3. Identified issues for LWLR.....	26
6.4. Future improvements for LWLR validation .....	27
6.5. LWLR references.....	27
7. Conclusions .....	31

## 1. Introduction

This report describes the methodology used to select the most suitable algorithms to produce the Lakes Essential Climate Variables (ECVs) from satellite observation. Furthermore, this report covers the initial validation of the resulting products and plans to evolve the underlying algorithms.

The selected algorithms are, in the case of most of the thematic Lakes ECVs, the result of research activities preceding the Lakes\_cci and leading up to the state-of-the-art introduced in the production system for Lakes\_cci. This is the status with regard to the production of version one of the Climate Research Data Package (CRDP V1).

Issues that are identified during algorithm selection and validation are subsequently addressed in the research and development period leading up to the second Climate Research Data Package (CRDP V2). Plans leading to improvement of specific algorithms, insofar as they are currently foreseen, are therefore given in this document.

The following sections are broken down first by thematic variable within the Lakes\_cci and subsequently into the following topics:

- Candidate algorithms - an overview of the algorithms selected for comparison
- Validation results to date - leading to algorithm selection for CRDP V1
- Identified issues - where further development and validation is considered necessary
- Future improvements - an overview of which additional algorithms, or changes in existing algorithms, shall be explored in the period leading up to CRDP V2

## 2. Lake Water Level (LWL) algorithms

### 2.1. Candidate algorithms for LWL

The algorithm for LWL calculation was developed at LEGOS and is detailed in the ATBD. It is based on the state-of-the-art in calculating LWL from satellite altimetry. Since each altimeter provides a distinct Global Data Record, an initial phase of organising the data and the geophysical corrections is required to produce a coherent climate data record. Moreover, each satellite mission presents a specific altimeter bias which requires correcting (based on published results), in order to arrive at a consistent long-term multi-satellite LWL time series.

The software used in this process has been previously developed and is named Hysope. It can be used operationally and is based on Intermediate Geophysical Data Records (IGDRs). It is operated at CLS in the framework of the Hydroweb database. A version for non-operational use also runs at LEGOS and is based on the same equations, but using Geophysical Data Records (GDRs) instead of IGDRs (Cretaux et al., 2016).

The procedure is run against data within a priori defined polygons of lake contours (using the common dataset of maximum water extent outlines created for Lakes\_cci) which are then processed using the Hysope software which is classically using the following equation:

$$\text{LWL} = \text{Alt} - \text{Rcorr} - \text{TE} \quad [2.1]$$

Where LWL is considered with respect to a geoid, Rcorr is the measured range between the satellite and the lake surface, Alt is the altitude of the satellite above an ellipsoid and TE is the combination of all correction factors to take into account atmospheric refraction (propagation in the ionosphere and the troposphere), tidal effects (solid Earth, lake and polar), and geoid height above the ellipsoid. For readers who needs more detailed information a full discussion of the computation of LWL is found in Cretaux et al. (2009).

All corrections are released in the GDRs or the IGDRs. The range is chosen from different retracking considering that generally the OCOG retracking is the most suitable for continental surface (see

E3UB document). The geoid correction is calculated using the repeat track technique (see E3UB and Cretaux et al. 2009, 2016).

## 2.2. Validation results for LWL

---

The general algorithm used to calculate water level over lakes is well known and established in scientific literature. To address the issues that are listed in the following sections, we need to analyse lakes where reference in situ data are available. Examples of these procedures are given in Ricko et al. (2012) and Arsen et al. (2015), comparing different lake databases.

Lakes\_cci cooperates with the State Hydrological Institute of St Petersburg, which provides in situ data of LWL for a set of Russian and central Asian lakes. We also use existing databases on the web to increase the number of lakes that can be used for this purpose.

The comparative analysis allows the statistically best performing retracking algorithm to be selected, as has been widely demonstrated for lakes as well as rivers.

Additional metrics to validate the LWL products include comparison of individual LWL retrieval to the long-term LWL variability, in order to detect outliers. The impact of removing outliers is traced as part of this process.

## 2.3. Identified issues for LWL

---

There are two main issues currently under investigation for processing of altimetry data over lakes. The first is related to the onboard tracking system, and the second is related to the processing of altimetry over small lakes.

We have identified solutions to address onboard tracking issues based on new a priori information. For retrieval of LWL over small lakes we identify solutions based in new algorithms for SAR data. Both approaches are detailed in section 2.4.

Another separate consideration of retrieval performance is the calculation of relative biases when several satellites of different types of orbit are used over a given lake. When we use a series of satellites such as Topex / Poseidon, Jason-1/2/3, we collect data from the same orbit, so that the relative bias between each mission is well described and calibrated (see Cretaux et al. 2009, 2011, 2013, 2018, Bonnefond et al., 2018). When observations from different orbit are used, however, such as with Jason and Envisat or Jason and Sentinel-3, another bias is added. The instrumental biases are known, but since the tracks do not cover the same position over the lake, an additional bias due to geoid error has to be considered. A very simple method has been developed at Legos to correct for this additional bias. The LWL is calculated independently using each track, over the whole period of time, and during the overlapping period we interpolate the point measurement from each pass and calculate the average difference between all interpolate points. It then corresponds to the additional bias due to geoid errors.

## 2.4. Future improvements for LWL

---

We have identified three main future improvements.

1. The LWL time series are based on long term time series of altimetry data. To achieve this goal, we process measurements from several satellites when it is possible. Currently the Topex / Poseidon, ERS2, and Jason-1 are processed using only classical retracking based on the algorithm tuned for ocean-type waveform. For many lakes it is therefore not precise enough to be included in the products. The issue particularly concerns small and medium size lakes. In the second phase of the project, in coordination with other projects and in accordance to the development's plan of Hydroweb, the waveform of these three satellites will be reprocessed using several retracking algorithm (OCOG, ICE-2, ICE-3). We expect from these reprocessing to first of all increase the number of lakes within the database, and secondly to also produce longer time series for existing lakes where only Envisat or Jason-2 / Jason-3 were processed. Length of time series of LWL is indeed essential in the

framework of climate change studies, in order to detect climate signal within time series constrained by different type of periodic and non-periodic fluctuations.

2. For small lakes, particularly in mountain areas (Andean chain, Tibetan Plateau, Alps) the onboard tracking algorithm often does not capture the echo since the observing gate of the altimeter is not tuned in advance to the absolute height of the target. To solve this problem, CNES has set up an a-priori database including reference height of many targets over continents: on rivers, and on lakes. Coupled with the onboard navigator (DIODE) which provides in advance the precise orbit of the satellite, it is possible to force the altimeter to switch the onboard tracker to the right gate, corresponding to the height of the target. The accuracy of reference height does not need to be very accurate, since a window of  $\pm 5$  meters is sufficient to capture the echo. LEGOS is building a Digital Elevation Model (DEM) including the reference height of thousands of lakes and rivers. This DEM will be uploaded to some active satellites: this has been tested with Jason-3 and led to a significant increase in the number of lakes and rivers now measurable from this satellite. It is planned to do the same with Sentinel-3A and Sentinel-3B missions, and also to include this DEM with future missions like Jason-CS.
3. Recent missions such as Sentinel-3 provide SAR data. One of the main advantages is to improve the resolution of the altimeter along the track. Using unfocused SAR processing techniques the resolution is improved by an order of magnitude compared to previous altimeters. It allows small-scale features over lakes and rivers to be captured more frequently and more accurately, particularly when their geometry is perpendicular to the satellite track.

A novel approach was recently developed (Egido and Smith 2017) which performs a coherent integration of the SAR echoes along the satellite track. This method works as long as the transmitted pulse remains coherent during the target illumination time. This method, called Fully Focused SAR processing, can achieve decimetre along-track resolution which is more than two orders of magnitude of improvement with respect to unfocused conventional approaches. The application of this method for hydrology in general and lake studies in particular is revolutionary. Potentially several thousands of new lakes and reservoirs will be observable in future. Plans are underway between CLS and Legos to implement this method for future use in Hydroweb. It will allow, before the end of Lakes\_cci, production of a new set of hundreds of lakes for LWL within the CCI database.

Validation of these novel approaches will follow the same principles as laid out above.

## 2.5. LWL References

---

- Arsen, A., JF. Cretaux, and R. Abarca-Del-Rio. 2015. Use of SARAL/AltiKa over mountainous lakes, intercomparison with Envisat mission J. of Adv. Space Res. The Saral/ALtiKa satellite Altimetry Mission, 38, 534-548,2015, doi: 10.1080/01490419.2014.1002590
- Bonnefond, P.; Verron, J.; Aublanc, J.; Babu, K.N.; Berge-Nguyen, M.; Cancet, M.; Chaudhary, A.; Cretaux, J-F.; Frappart, F.; Haines, B.J. , Laurain, O.; Ollivier, A.; Poisson, J.C.; Prandi, P.; Sharma, R.; Thibaut, P.; Watson, C. The benefits of the Ka-Band as evidenced from the SARAL/AltiKa Altimetric mission: quality assessment and unique characteristics of AltiKa data, Remote Sensing. 2018, 10(1), 83, doi:1039/rs/10010083
- Cretaux, J.F., S. Calmant, V. Romanovski, et al. 2009. An absolute calibration site for radar altimeters in the continental domain: lake Issykkul in Central Asia, Journal of Geodesy 83 (8) 723-735 DOI: 10.1007/s00190-008-0289-7
- Cretaux, J.F., S. Calmant, V. Romanovski, et al. 2011 Absolute Calibration of Jason radar altimeters from GPS kinematic campaigns over Lake Issykkul, Marine Geodesy, 34 : 3-4,291-318, DOI: 10.1080/01490419.2011.585110
- Crétau J-F., Bergé-Nguyen M., Calmant S., Romanovski V.V., Meyssignac B., Perosanz F., Tashbaeva S., Arsen A., Fund F., Martignago N., Bonnefond P., Laurain O., Morrow R., Maisongrande P., 2013 Calibration of envisat radar altimeter over Lake Issykkul, J. Adv. Space Res., Vol 51, 8, 1523-1541, doi: 10.1016/j.asr.2012.06.039

- Cretaux J-F, M. Bergé-Nguyen, S. Calmant, N. Jamangulova, R. Satylkanov, F. Lyard, F. Perosanz, J. Verron, A.S. Montazem, G. Leguilcher, D. Leroux, J. Barrie, P. Maisongrande and P. Bonnefond, 2018, Absolute calibration / validation of the altimeters on Sentinel-3A and Jason-3 over the lake Issykkul, *Remote sensing*, 10, 1679,; doi:10.3390/rs10111679
- Egido A., and W.H.F Smith, 2017, Fuly Focus SAR altimetry: Theory and applications, *IEEE*, 55, 1
- Ričko M., C.M. Birkett, J.A. Carton, and J-F. Cretaux, Intercomparison and validation of continental water level products derived from satellite radar altimetry, *J. of Applied Rem. Sensing*, Volume 6, Art N°: 061710, DOI: 10.1117/1.JRS.6.061710, 2012

### 3. Lake Water Extent (LWE) algorithms

Both optical and SAR data are used to estimate LWE. Since the processing chains for the two sensors differ, candidate algorithms are described separately in the following sections. The first section focuses on the optical approach, followed by SAR-based algorithm considerations. These algorithms are currently under development - additional detail is given in the ATBD.

#### 3.1. LWE-optical approach

##### 3.1.1. Candidate algorithms for the LWE-optical approach

Based on results and recommendations from the CNES-funded R&T project “Extraction of information from multi-source flows, applied to water surfaces”, an unsupervised approach (Otsu 1979) and two supervised algorithms, SVM and Random Forest, were selected for evaluation.

Thresholding is one of the most basic classification methods. From a grey scale image, a value is computed as the limit between two or more classes. The Otsu (1979) method allows an optimal threshold to be selected by reducing the within-class variance, or by maximizing the between-class variance. This method has a simple implementation with corresponding advantages for computation requirements.

Support-vector machines (SVMs, also support-vector networks) are supervised learning models with associated learning algorithms that analyse data used for classification and regression analysis. Given a set of training examples, each marked as belonging to one or the other of two categories, an SVM training algorithm builds a model that assigns new examples to one category or the other, making it a non-probabilistic binary linear classifier. An SVM model is a representation of the examples as points in space, mapped so that the examples of the separate categories are divided by a clear gap that is as wide as possible. New examples are then mapped in the same space and predicted to belong to a category based on which side of the side gap they fall.

Random forests or random decision forests are an ensemble learning method for classification, regression and other tasks that operates by constructing a multitude of decision trees. Important concepts of RF are bagging (bootstrap aggregating) and Out-of-bag error (OBB). The bootstrap sampling allows for the decorrelation of the trees and therefore improves the results and the robustness of the model. The OBB error can be used to determine the importance of features used for the training.

##### 3.1.2. Existing validation results for the LWE-optical approach

Our validation procedures include inter-comparison of results and an analysis of the derived LWE over a set of selected case studies over several years. This inter-comparison allows a semi-qualitative ranking of candidate methods and it highlights their limitations in terms of performance due to local conditions (environment, weather, ice/snow, etc) and experimental conditions (training set selection procedures, inputs qualities).

Validation of individual LWE results is subject to ongoing discussion. Lake water masks should be compared with an accurate reference LWE which can come from a ground truth campaign (very rare) or a ground truth proxy (photo interpretation on higher resolution data). The critical parameter of the reference layer (used for validation) is the temporal difference between its source date and the acquisition date analysed. In fact, the same water dynamics must be compared. The difficulty increases with lake size. A solution is to first work on smaller lakes up to intermediate scales of a few hundred km<sup>2</sup>. At these scales, VHR1 or VHR2 satellite images can be acquired and the LWE derived from this metric or infra metric images can serve as a reference. This is conceptually simple but has the following practical restrictions:

- HR and VHR images must be acquired on the same day or with the shortest possible delay (i.e. within a few days). Works done in other project have highlighted this requirement suggesting that two days can already be too long.
- The optical images exploited as reference and slave data need to be spectrally coherent, covering the same domains. Most of the approaches for Sentinel-2 or Landsat data exploit primitives, raw SWIR channels, or indices (MNDWI, NDWI, AWEI) derived from these SWIR channels, whereas the VHR data do not cover the full spectral domain, being restricted to VIS and NIR.
- Reduced confidence in water extraction based on automated approaches compared to visual interpretation of the imagery, particularly over low water levels. With low water depth the reflected signal can become associated with the lake bottom rather than the water itself. In addition, the definition of the limits between water and wet muddy/sandy banks may not always be obvious. Visual interpretation is then necessary but this is not pragmatic given the effort, experience and knowledge required and difficulty of reproducibility.

Over Colhue Lake (Argentina) and Altevatnet (Norway) a set of SPOT6-7 imagery has been identified containing a few images of each lake. These data will be exploited to validate both the optical and SAR approach.

Within Lakes\_cci a third approach of validation is carried out based on the analysis and inter-comparison of derived hypsometric curves. The idea is that, when comparing LWE derived with different methodological /sensors approaches the best water times series would produce the best hypsometric curves and therefore statistical correlation can be used to corroborate the method.

### 3.1.3. Identified issues for the LWE-optical approach

The accuracy of the LWE estimates is found to be highly dependent on the type of lake and meteorological conditions during the image acquisition. For simple cases where the lake is well filled and close to its maximum extent and the satellite image is acquired with optimal meteorological conditions (e.g. little or no cloud cover), the results obtained by the different approaches are very similar. In the case of shallow water bodies, a large proportion of the reflected signal could originate from the bottom of the lake rather than from the water surface itself, leading to greater differences in LWE estimates between the different procedures. This may also occur in the case when the lake/water body has a high content of suspended material.

- Algorithm 1, SVM: More stable approach, sensitive to the training set selection and dependent on the input database exploited for the training set selection.
- Algorithm 2, Random Forest: Improves the generalization of the pre-trained, performs well under different image acquisition conditions.
- Algorithm 3, OTSU: analyses the dependency of floating / submerged / wetland vegetation.

Further validation will be needed for the following:

- Algorithm 2, Random Forest: further exploit the probability map associated with each derived water extent map.
- Shallow water application domain: exploitation of VHR imagery may help to address this complex case. This would help to respond at least partially to this case associated with hypsometric approach. Therefore, when water has completely redrawn

- Submerged/floating vegetation application: since the satellite imagery is sensitive to the properties of the targets, the detected lake water extent is dependent on how the target is defined i.e. whether the lake water extent is defined as only open water, or whether it should also include water bodies that are highly vegetated and contain targets that are not associated with only open water. It may be better to extract a minimum water extent that represents only the open water part of such water bodies or extend the definition to include all areas where water is present and dominant, including potentially large areas of wetlands.

### 3.1.4. Future improvements for the LWE-optical approach

Thus far, for LWE optical approach SVM appears to provide a reliable and consistent approach and this despite, as applied on optical imagery, its sensitivity to cloud cover. Improved detection of clouds or the exploitation of ancillary data such as the SAFE mask from Colorado Boulder University, can be tested. Should such cloud screening be successful then it can be equally applied to the OTSU and RF processing chains.

Concerning the Otsu threshold, an improvement based on Canny's edge detection algorithm could be implemented and tested (Donchyts et al. 2016). This added feature would focus on the calculation of the histogram over regions with strongly defined edges, which is the expected case at the interface between surface water and land. By doing so, the water signature becomes more strongly represented in the histogram resulting in a bimodal distribution and thus allows for a more adaptive threshold.

The Random Forest approach could be improved in various ways:

- Use of more training data for each Sentinel-2 tile in the time series. For example, rather than exploiting a single image of the tiles to derive the training set, and adjust the applied model, may derived for each image (or set of images with similar acquisitions parameters in term of year's period for example) specific training set and deriving models
- Fine tune the parameters of the Random Forest (number of trees, size of the leaf, ...)
- Take advantage of the probability map produced with each classification: this would allow for identification of regions where the detected water is more probable than others, leading to more accurate delimitation of the water bodies. This could be done by adjusting of the probability level, for example for shallows water extent the range of probability whereas for a "classical lake" be more restrictive
- Integrate deep learning techniques, especially semantic segmentation (Wieland et al., 2019).

### 3.1.5. LWE-optical references

Donchyts, G., Schellekens, J., Winsemius, H., Eisemann, E., & van de Giesen, N. (2016). A 30 m Resolution Surface Water Mask Including Estimation of Positional and Thematic Differences Using Landsat 8, SRTM and OpenStreetMap: A Case Study in the Murray-Darling Basin, Australia. *Remote Sensing*, 8(5), 386. doi:10.3390/rs8050386

Otsu, N. (1979). A threshold selection method from gray-level histograms. *IEEE transactions on systems, man, and cybernetics*, 9(1), 62-66.

Wieland, M., Martinis, S., and Li, Y.: Semantic segmentation of water bodies in multispectral satellites images for situational awareness in emergency response. *Int. Arch. Photogramm. Remote Sens. Spatial Inf. Sci.*, XLII-2/W16, 273-277, <https://doi.org/10.5194/isprs-archives-XLII-2-W16-273-2019>, 2019

### 3.2. LWE-SAR approach

#### 3.2.1. Candidate algorithms for the LWE-SAR approach

This section provides an overview of the methods tested by TRE-Altamira and NORCE. Details on the methods are given in the ATBD document, which also details how the methods should converge into a single processing scheme. Validation of the individual methods is used to determine approaches to overcome uncertainties in either method. These solutions can be considered candidates for implementation in the final SAR processing scheme.

The **TRE-Altamira Initial Methodology** operates over four different stages: pre-processing, water mask thresholding, image classification and results generation (Figure 1).

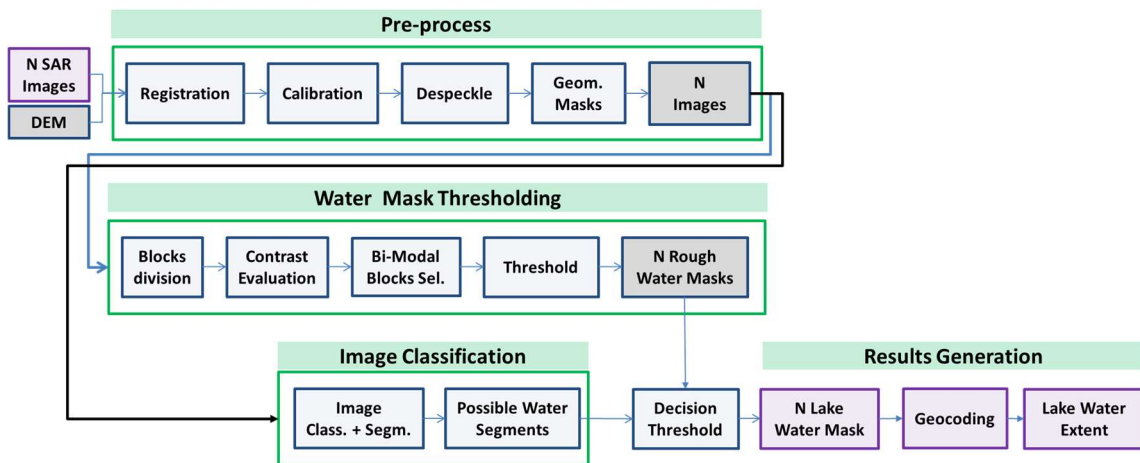


Figure 1 Initial TRE-Altamira methodology to test the Lake Water Extent using SAR images.

The **NORCE Initial Methodology** operates in three stages: pre-processing, water detection and post-processing (Figure 2).

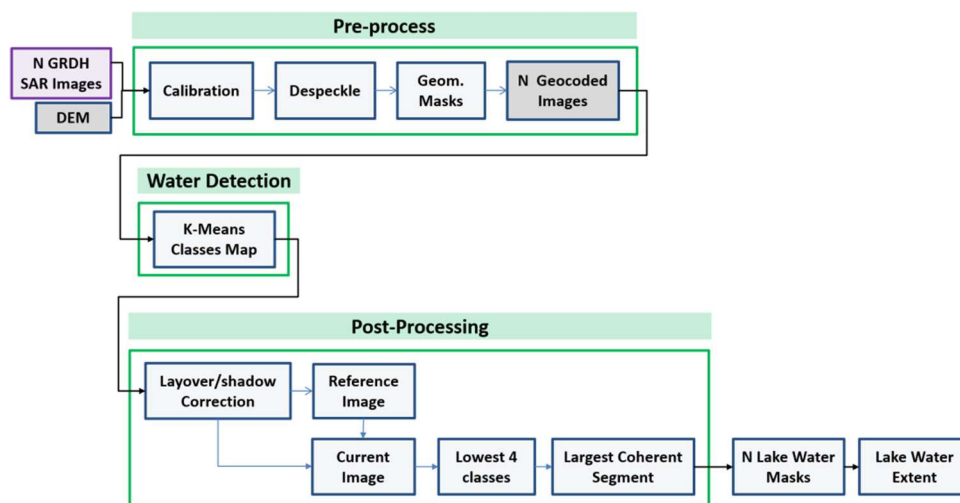
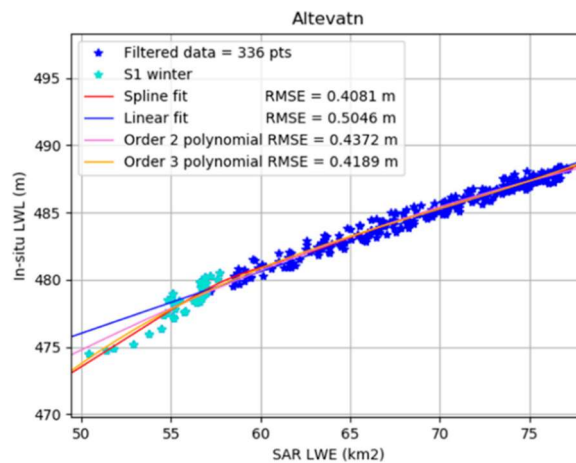


Figure 2 Initial NORCE methodology to test the Lake Water Extent using SAR images.

### 3.2.2. Existing validation results for the LWE-SAR approach

The existing validation results are based on the generation of the hypsometric curve derived from the SAR LWE time-series against LWL (acquired from an altimeter or measured in-situ). NORCE performed this kind of analysis on the Altevatn lake (Vickers et al. 2019) illustrated in Figure 3, showing the hypsometric curve employing different curves from Sentinel-1 LWE estimates vs in situ LWL. This study confirms that having a significantly populated time-series allows a fair assessment of the quality of the data.



**Figure 3** Scatter plot of the Sentinel-1 LWE estimates vs. corresponding in-situ measurements of lake water level, shown together with fitted natural spline function, polynomials of the first, second and third order, and the respective RMS in the LWL estimates.

### 3.2.3. Identified issues for the LWE-SAR approach

- On selected blocks with lower contrast the KDE threshold is not always properly calculated. This leads to a wrong selection of candidate K-Means segments, which significantly increases the false positive ratio, these being specially concentrated in the lake contours. At the same time, if increasing the contrast threshold, the density of selected blocks could be low adding more uncertainty to the threshold calculation. This issue was found in TRE-Altamira methodology.
- The number of classes belonging to the water class may vary depending on the lake or the diversity of the land cover surrounding the lake. This presents difficulties for automating the selection of K-means classes corresponding to water. This issue was found in both the TRE-Altamira and Norce methodologies.
- Kittler and Illingworth's and Otsu methods yield in general terms the same performance as the Kernel Density Estimator (even slightly worse), that is, they are deeply conditioned by the contrast in the analysed block. This issue was found in TRE-Altamira methodology.
- Cross and co-polar images can be exploited to maximize the results quality. It has been observed that especially at the land/water edge they show differences that can be exploited to better retrieve the lake limits. This issue was found in both methodologies.
- The entropy and the root mean square contrast operators show low values on water compared to the outer areas. The corresponding low lake values are distinguishable in both histogram images. This allows a threshold to be applied to select water pixels, provided that the inherent loss of spatial resolution on those operators prevents retrieval of the full extension so complementary steps are needed. This can be exploited to calculate the classes belonging to water. This issue was found after some preliminary tests done by both teams not being part of their strict processing chain.

- Morphological Snakes show promising results but parameter tuning is required in order to achieve the best accuracy. This issue was found after some preliminary tests done by both teams not being part of their strict processing chain.
- Sobel and Canny edge detectors yield interesting results. Nevertheless, fine tuning is also required and performances strongly depend on the presence of noise in the image. This issue was found after some preliminary tests done by both teams not being part of their strict processing chain.
- Ice and snow can be present on lakes in a significant part of the year. In that case, the presented methodologies do not hold, since the reflected radar signal from snow and ice is very different from that associated with water. As a result, those images are discarded. Therefore, at least in the present time, a gap in the lake water extent time series will be present. This issue is mainly related to the SAR image properties.
- Rough water surface, e.g. due to wind-induced waves and shallow waters can lead to misclassification since the SAR image backscatter values increase. Vegetation in the lake can have similar effects on the result.

### 3.2.4. Future improvements for the LWE-SAR approach

As explained in the previous section, some methodologies are preferable for exploitation in order to increase the quality of the extracted lake water extent. Further characterization and testing are needed on them.

The combination of polarimetric information, for example use of both cross and co-polar images in the case of Sentinel-1, is identified to be one of the improvements that should be done in the future. This applies in particular to the definition of the lake outline definition, where different behaviour in the backscattered SAR signal associated with the two polarizations can be exploited.

Speckle filter on the amplitude SAR images is also something to consider as a future improvement.

A test using an Artificial Intelligence approach will be performed. The idea will be to use previous results from K-means classification (with manual quality inspection) as training data.

A systematic exploitation of the entropy and root mean square contrast operators will be explored. The use of Morphological Snakes will be also included.

Improvement on automation should also be considered. Many processing steps and operators work considering a spatial analysis on the images. Elements as the spatial analysis block size has to be automatically adapted to a particular lake.

Particular attention has to be focused on the error budget characterization. Classification methods are part of the processing core of the described methodologies, but present difficulties in providing an error estimate for each pixel. Work on this characterization has to be considered in future steps.

In the present time, some SAR images have to be discarded when the SAR backscatter is affected by elements such as wind, ice and snow. A step further would be to develop methodologies for ice and snow detection to characterize the lake water extent among these conditions. In any case, a proper definition itself on what lake water extent means in those cases would be required.

In summary the expected outcome would be a SAR processing chain that maximizes the lake water extent quality among the largest types of lakes according to their environmental conditions.

### 3.2.5. LWE-SAR references

S. Martinis, A. Twele, and S. Voigt. , “Towards operational near real-time flood detection using a split-based automatic thresholding procedure on high resolution TerraSAR-X data”, *Nat. Hazards Earth Syst. Sci.*, 9, 303-314, 2009.

S. Martinis and R. Christoph, “Backscatter Analysis Using Multi-Temporal and Multi-Frequency SAR Data in the Context of Flood Mapping at River Saale, Germany”. *Remote Sensing*. 2015, 7(6), 7732-7752.

L. Landuyt, A. Van Wesemael, G. J. -. Schumann, R. Hostache, N. E. C. Verhoest and F. M. B. Van Coillie, "Flood Mapping Based on Synthetic Aperture Radar: An Assessment of Established Approaches," in *IEEE Transactions on Geoscience and Remote Sensing*, vol. 57, no. 2, pp. 722-739, Feb. 2019.

H. Vickers, Eirik Malnes, K-A Hodga. "Long-term Water Surface Area Monitoring and Derived Water Level using Synthetic Aperture Radar (SAR) at Altevattn, a Medium-Sized Arctic Lake". *Remote Sens.* 2019, 11(23), 2780.

## 4. Lake Surface Water Temperature (LSWT) algorithms

### 4.1. Candidate algorithms for LSWT

Surface temperatures from infrared observations are obtained by coefficient-based methods or optimal estimation (OE, Merchant and Embury 2014). Because of the varied altitudes of lakes and the large differences in atmospheric absorption associated with continentality, optimal estimation is the appropriate approach for LSWT estimation (MacCallum and Merchant, 2012).

OE also provides comprehensive equations for uncertainty evaluation, on which basis uncertainty estimates are provided in LSWT products per datum.

As well as retrieval, classification of which pixels are filled with water under clear skies is a necessary part of the LSWT processing. This is done by a "fuzzy logic" style approach in which a number of metrics with fuzzy thresholds are combined into a "water detection score" that contributes to the definition of the quality level attributed to the pixel. Bayesian cloud detection, as used for sea surface temperature, was also considered to identify clear-sky pixels but is heavily compromised in its current implementation for small lakes, where the spatial coherence of the temperature of the scene is not a good indicator of cloud (unlike in the centre of large lakes and over open ocean). Because of the user requirement to increase the number of measured lakes, the latter scheme is therefore currently inapplicable for the identification of clear-sky only water pixels.

### 4.2. Existing validation results for LSWT

Validation results (for LSWT 4.0, the pre-CCI version) are summarised in the E3UB. The validation undertaken is a comparison of satellite to matched in situ temperatures. These comparisons are limited by the non-representative sample-of-opportunity (in situ measurements being unfortunately hard to obtain) and by variable and often unknown in situ uncertainty characteristics and quality control. Validation results are too ambivalent in this case to be used as a discriminant between alternative algorithmic approaches, and for LSWT are not used in this way. As mentioned in the previous section, the retrieval algorithm is established by considerations rooted in physics and inverse theory.

Nonetheless, the validation exercise is sufficient to establish that for quality level (QL) 5 (best quality) LSWT data, the data have low bias (<0.1 K) and uncertainty estimates are reasonable.

### 4.3. Identified issues for LSWT

#### LSWT retrieval

1. Optimal estimation uses an observation-simulation error covariance matrix. This matrix is presently a simple diagonal estimate that doesn't account for the likelihood of cross-channel correlations in the simulation errors.
2. Optimal estimation uses a prior error covariance matrix. This matrix is a simple diagonal estimate based on experience of ERA-interim, and ideally should be updated for use with ERA-5.

### LSWT retrieval uncertainty

(NB, this aspect is also addressed by the issues identified for LSWT retrieval.)

1. The decomposition of the optimal estimation uncertainty into different correlation length scales is an approximation; a more complete solution needs to be coded. (The decomposition is relevant when creating gridded data.)

### Water detection

1. The water detection to select water-only pixels relies on day time (reflectance) channels, and therefore cannot be applied at night. The alternative that may work at night is based on Bayesian cloud screening (as used in SST CCI), but for small lakes would require considerable research, development and modification.

### Quality level determination

1. QL determination is based mainly on water detection results and also on retrieval chi-square results (which measure the plausibility of the solution given the prior and observations). However, the chi-square results differed more than expected between Metop-A and Metop-B AVHRRs, affecting the QL attribution adversely in the case of Metop-B. This is yet to be understood.

### Increasing coverage using MODIS

1. By far the most impactful issue for users for LSWT is to increase the density of coverage, which is limited by sensor-orbit coverage and by cloud cover. The most practicable approach is to add MODIS to the processed data streams. This will involve creating water detection and retrieval parameters analogous to those for the ATSRs and AVHRRs, testing and implementing the retrieval.
2. MODIS offers additional capabilities such as higher visible resolution in some channels and additional thermal channels, particularly at 8.7 um. With these capabilities, as well as adding coverage, MODIS may facilitate single-view retrievals with lower uncertainty.

### Implications for LSWT v4.1 (Lake CCI version 1)

LSWT v4.1 will have additionally Metop-B, which greatly increases the coverage for users, but not yet MODIS. A work-around for the Metop-B issue with chi-square is implemented, but a more fundamental resolution will still be pending in this version.

LSWT v4.1 will use ERA-Interim for the background numerical weather prediction data and will continue to be based on day-time images.

## 4.4. Future improvements for LSWT

---

For version LSWT v5.0 (Lake CCI v2):

1. The issue of error covariance estimation for optimal estimation is a long-standing problem, to which a possible solution (Merchant et al., 2019) has recently been proposed. These techniques will be applied within SST CCI and the matrices will be applicable for LSWT v5.0.
2. The approximations in the uncertainty decomposition will be removed and a more exact solution implemented.
3. MODIS will be added to the processed data stream, either on the same algorithmic basis as Metop AVHRRs, or with additional improvements using MODIS capabilities if research yields these in time (particularly, exploitation of the 8.7 um channel).
4. LSWT v5.0 will have switched from ERA-interim to ERA-5 for background numerical weather prediction information. However, the optimisation of associated error covariance information will not have been undertaken. Moreover, the known improvements to the detail of the uncertainty evaluation are also planned for later. Therefore, the v4.0 and v4.1 approximations to the LSWT uncertainty estimates will persist in v5.0.

Beyond LSWT v5.0:

1. The LSWT record would greatly benefit from inclusion of night-time data, which are possible for the large lakes in the "ARC-lake" project, but for which no solution exists for

small lakes within our target population. This is a hard problem, that may rely on building up detailed knowledge and databases lake-by-lake. The R&D resources within the Lake CCI programme are insufficient for this scale of development in this phase, because 5 distinct variables are treated within one project.

2. The U.S. successor to MODIS and AVHRR is the VIIRS series, which will be excellent for LSWT coverage and quality. However, we have no practicable (affordable) means of accessing the data stream presently. We have approached NOAA/NASA about whether CCI processing can be run at source on their data, but a framework for this is yet to be found. We will continue to pursue this.

#### 4.5. LSWT References

---

MacCallum, S.N. and Merchant, C.J. (2012) Surface water temperature observations of large lakes by optimal estimation. *Canadian Journal of Remote Sensing*, 38 (1). pp. 25-45. ISSN 1712-7971 doi: <https://doi.org/10.5589/m12-010>

Merchant, C. J. and Embury, O. (2014) Simulation and inversion of satellite thermal measurements. In: Zibordi, G., Donlon, C. J. and Parr, A. C. (eds.) *Optical radiometry for ocean climate measurements. Experimental methods in the physical sciences*, 47 (47). Academic Press, pp. 489-526. ISBN 9780124170117 doi: <https://doi.org/10.1016/B978-0-12-417011-7.00015-5>

Merchant, C., Saux-Picart, S. and Waller, J. (2019) Parameters for optimal estimation by exploiting matched in-situ references. *Remote Sensing of Environment* 237, 111590.

### 5. Lake Ice Cover (LIC) algorithms

---

#### 5.1. Candidate algorithms for LIC

---

The LIC retrieval algorithm selected for Lakes\_cci CDR v1 production relies on a threshold-based approach that consists of two parts; one for cloud detection (cloud-covered or cloud-free pixels) and the other for ice detection (ice-covered or open water pixels). The set of criteria and threshold values implemented for Lakes\_cci have been devised to retrieve these classes (ice cover, open water and cloud cover) based on the MODIS Terra/Aqua Atmospherically Corrected Surface Reflectance 5-Min L2 Swath (MOD09/MYD09), Collection 6, product (Vermotte et al., 2015). An earlier version of the retrieval algorithm ingested MODIS Level 1B Calibrated Radiances (TOA reflectance; MOD02/MYD02 product) instead, as is currently done for the generation the MODIS (Terra only) lake ice extent 250-m product for Northern Europe by the Copernicus Global Land Service.

In the threshold-based approach using either MOD09/MYD09 or MOD02/MYD02, a modified version of the Simple Cloud Detection Algorithm (SCDA) proposed by Metsämäki et al. (2011) is used to detect cloud-covered and cloud-free pixels. The SCDA uses a combination of visible, mid-infrared and thermal bands - MODIS bands 4, 6 (replaced by band 7 for MODIS Aqua due to band 6 detector problems), 20, 31 and 32. The second part of the algorithm, also threshold-based, detects ice cover and open water for pixels flagged as cloud-free. This part of the algorithm uses MODIS bands 2, 3 and 4. A detailed description of the algorithm and bands used in the retrieval process is provided in the Algorithm Theoretical Basis Document (ATBD).

The algorithm that uses MOD09/MYD09 (surface reflectance) as input has been found to outperform the one that utilizes MOD02/MYD02 (TOA reflectance) and, hence, is the one adopted for Lakes\_cci v1. Validation results of the threshold-based approach using MOD09/MYD09 and MOD02/MYD02 as input are presented next.

#### 5.2. Validation results for LIC

---

The LIC retrieval algorithm has been developed and validated through a detailed examination of surface reflectance (and brightness temperature) over ice, open water and cloud cover under

various conditions (e.g. thin ice, turbid water, thin clouds, high solar zenith angles) during both the break-up (BU) and freeze-up (FU) periods from a selection of 17 large lakes across the Northern Hemisphere (North America and Eurasia) (Figure 4).

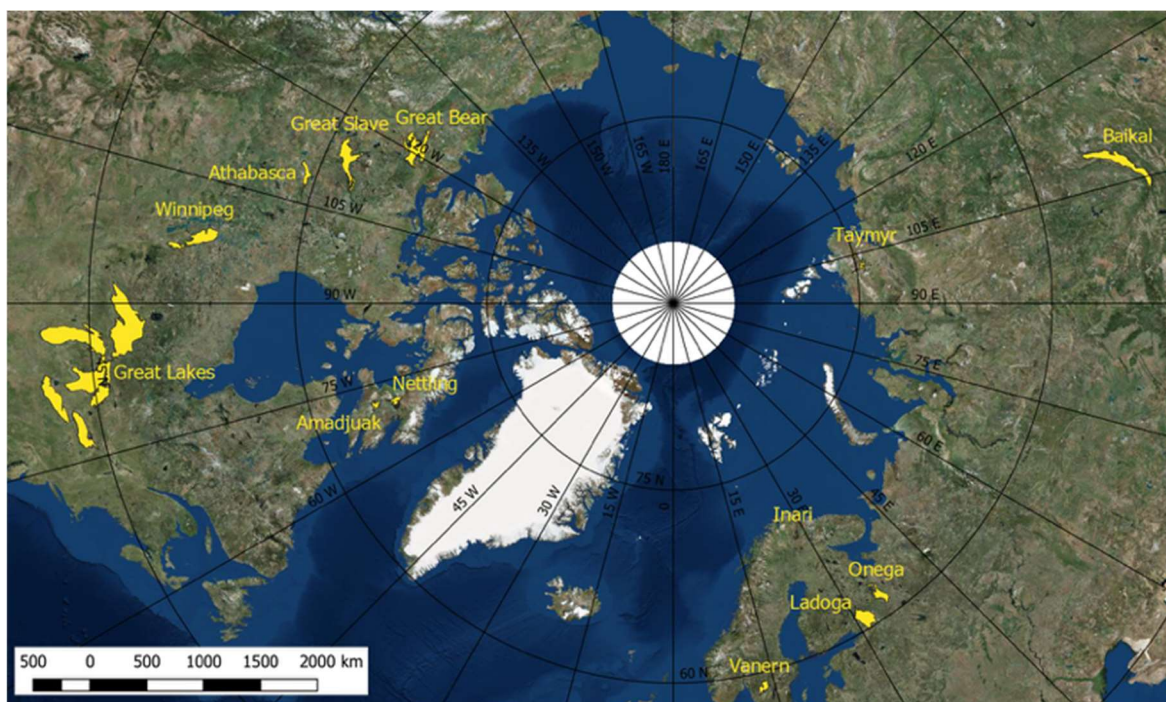


**Figure 4: Geographical distribution of 17 lakes used for Lakes\_cci LIC v1 algorithm development and validation**

An accuracy assessment has been performed for LIC products derived from the algorithm selected for Lakes\_cci (referred to as Lakes\_cci LIC) using MOD09/MYD09 surface reflectance and MOD02/MYD02 (TOA reflectance), both based on MODIS Collection 6 data. The confusion matrices presented below (Table 1 and Table 2) were produced using 165,697 test pixels from AOIs collected through visual interpretation of 108 images (MODIS Aqua and Terra at 17 lakes) acquired during both the BU (68 images) and FU (40 images) in ice seasons 2002-2003, 2009-2010, and 2016-2017.

Table 1 shows the overall accuracy (OA) of the two products (break-up and freeze-up periods combined). The algorithm selected for Lakes\_cci that uses MOD09/MYD09 provides the highest overall accuracy (95.54%), and also for individual classes (91.71% for ice cover, 98.85% for water, and 95.63% for cloud cover) compared to retrievals based on MOD02/MYD02.

Table 2 shows the accuracies reached using MOD09/MYD09 (surface reflectance) and MOD02/MYD02 (TOA reflectance) for the BU and FU periods taken individually. There is no notable difference in the accuracy of Lakes\_cci LIC (MOD09/MYD09) between the BU (OA: 95.80%) and FU (OA: 95.12%) periods, and the classification accuracies are consistent across classes. The LIC product generated with MOD02/MYD02 as input performs comparably well during the BU period, but poorly during the FU period. The lower performance of the threshold-based algorithm using TOA reflectance has been found to be particularly revealing for high-latitude lakes when solar zenith angles are large (ca.  $\geq 70$  degrees).

**Table 1: Confusion matrices with retrieval accuracies for Lakes\_cci LIC (MOD09/MYD09) and MOD02/MYD02 LIC products (break-up and freeze-up periods combined)**

Lakes_cci LIC		Retrieval Algorithm			Accuracy
		Ice	Water	Cloud	
User-defined	Ice	46968	2737	1510	91.71%
	Water	506	57435	165	98.85%

	Cloud	2272	192	53912	95.63%
Overall Accuracy: 95.54%					
MOD02/MYD02 LIC		Ice	Water	Cloud	Accuracy
User-defined	Ice	35275	13944	2130	68.70%
	Water	42	57862	35	99.87%
	Cloud	2397	11387	42625	75.56%
Overall Accuracy: 81.93%					

**Table 2: Confusion matrices with retrieval accuracies for Lakes\_cci LIC (MOD09/MYD09) and MOD02/MYD02 LIC products (break-up and freeze-up periods individually)**

		Break-Up				Freeze-Up			
		Retrieval Algorithm				Retrieval Algorithm			
Lakes_cci LIC		Ice	Water	Cloud	Accuracy	Ice	Water	Cloud	Accuracy
User-defined	Ice	29128	2535	133	91.61%	17840	202	1377	91.87%
	Water	16	39520	47	99.84%	490	17915	118	96.72%
	Cloud	1418	162	29750	94.96%	854	30	24162	96.47%
Overall Accuracy: 95.80%					Overall Accuracy: 95.12%				
MOD02/MYD02 LIC		Ice	Water	Cloud	Accuracy	Ice	Water	Cloud	Accuracy
User-defined	Ice	29084	2306	408	91.46%	6191	11638	1722	31.67%
	Water	42	39481	18	99.85%	0	18381	17	99.91%
	Cloud	1272	618	29480	93.98%	1125	10769	13145	52.50%
Overall Accuracy: 95.46%					Overall Accuracy: 59.88%				

### 5.3. Identified issues for LIC

While validation results of the Lakes\_cci LIC retrieval algorithm obtained to date are promising (errors to be less than 10% based on 17 lake sites), a few issues warrant further investigation.

1. Cloud cover: Cloud detection is improved with the SCDA algorithm implemented for Lakes\_cci compared to NASA’s MOD35/MYD35 product. However, a broader assessment of algorithm performance for the detection of thin clouds in both space (more lakes) and time (more timestamps) is needed.
2. Solar zenith angle: Using MODIS surface reflectance (MOD09/MYD09) as input rather than TOA reflectance (MOD02/MYD02) results in more accurate retrievals for high-latitude lakes where solar zenith angles are large for extended periods of time during the ice season. Validation needs to be performed over a larger number of lakes and ice seasons than what has been accomplished to date.
3. Water detection: Water detection is not implemented in the current version of Lakes\_cci LIC retrieval algorithm. As a result, a dry lakebed could be mistakenly classified as ice covered in summer due to high reflectance of such surface compared to open water. This issue is expected to be minor “globally”, but one that still needs to be addressed to ensure high retrieval performance for all regions of the globe.
4. Uncertainty: Pixel-level uncertainty is currently provided from overall classification errors calculated for each of the three classes (ice cover, open water and cloud cover) reported in Table 1. All individual sources of uncertainty have yet to be fully characterized and quantified.

## 5.4. Future improvements for LIC

---

Of the issues identified in Section 5.3, water detection as well as more complete characterization and quantification of uncertainty will be addressed first in the period leading up to CRDP V2. Issues related to the detection of thin clouds and the impact of large solar zenith angles on LIC retrieval performance will also be considered for the next version of the algorithm, once feedback has been received from data users of CRDP V1.

One major effort planned in the period leading to CRDP V2 is an evaluation of machine learning (ML) classifiers for LIC retrieval from MODIS, VIIRS and Sentinel-3 TOA reflectance (level 1) data. Of the ML classifiers, five are currently being tested on MODIS MOD02/MYD02 for the selection of lakes shown in Figure 4: multinomial logistic regression, support vector machine, random forest, gradient boosting trees, and convolutional neural networks. While the threshold-based approach adopted to generate CRDP V1 showed better overall LIC retrieval performance from MODIS surface reflectance (level 2) rather than TOA reflectance (level 1) data as input, ML classifiers may perform equally well using TOA reflectance. Indeed, early results indicate that classification accuracies as high as 98-99% may be achievable (Wu et al. *in prep.*; Wu et al. *in review*).

## 5.5. LIC References

---

Metsämäki, S., Sandner, R., Nagler, T., Solberg, R., Wangensteen, B., Luojus, K., et al. (2011) Cloud detection algorithm SCDA. GlobSnow Technical Note 2. European Space Agency.

Vermote, E. F., Roger, J. C., & Ray, J. P. (2015) MODIS surface reflectance user's guide collection 6. Maryland: MODIS Land Surface Reflectance Science Computing Facility.

Wu, Y., Duguay, C. R., & Xu, L. (in review) Lake ice classification from MODIS TOA reflectance imagery using a convolutional neural network: a case study of Great Slave Lake, Canada. Proceedings of 2020 IEEE International Geoscience & Remote Sensing Symposium, Waikoloa, Hawaii, USA, 19-24 July, 4 pp.

Wu, Y., Duguay, C. R., & Xu, L. (in preparation) Mapping lake ice cover from MODIS using machine learning approaches.

## 6. Lake Water Leaving Reflectance (LWLR) algorithms

---

### 6.1. Candidate algorithms for LWLR

---

Algorithms in the LWLR processing chain *Calimnos* chain fall into three categories:

- Pre-processing including pixel identification as water, land, cloud and ice
- Atmospheric correction yielding LWLR
- Retrieval of derived water-column properties, notably chlorophyll-a and turbidity

For the **pre-processing** category the processor relies on the Idepix multi-sensor processor in SNAP. The algorithm combines information from static sources (such as water extent) and dynamic pixel identification based on a neural network trained for each of the optical sensors. Depending on the capabilities of the sensor, the processing chain will rely on combinations of these processes. The algorithm is not part of validation of the Lakes\_cci LWLR but its performance is taken into consideration with regard to consistency in water/land masking between the Lakes\_cci thematic ECVs.

Validation of algorithms for **atmospheric correction** requires near-coincident in situ observations of water-leaving reflectance. Due to scarce in situ data from lakes, the window of acceptable coincidence may be up to several days from satellite observation. Longer time windows allow more data points to be included, which is suitable to determine the best-performing algorithm but less suitable to determine product uncertainties which may be exaggerated. The majority of

radiometric in situ data for lakes deposited in LIMNADES, the largest and only community-owned repository for lake bio-optical measurements, correspond to the MERIS observation period. Therefore, the procedure for selecting and evaluation of candidate algorithms is as follows:

- Round-robin evaluation of MERIS atmospheric correction algorithms
- Application of the most suitable MERIS algorithm(s) to MERIS and OLCI
- Evaluation of algorithms for MODIS based on minimizing inter-sensor bias during overlap with MERIS and OLCI, respectively
- A strategy for including SeaWiFS observations will be defined based on the results of MODIS (and VIIRS).

Finally, **algorithms for the derived water-column properties**, notably chlorophyll-a and turbidity (either directly or by conversion of total suspended matter concentration, usually following Nechad et al. 2016), are evaluated in a sensor-dependent manner similar to the procedure given for atmospheric correction algorithms. These algorithms are first evaluated against the available in situ data archives to assess their application range. The algorithms are then tuned for optimal performance as a function of their membership to a set of **optical water types**, allowing them to be mapped to satellite imagery using a weighted averaging ‘blending’ method. Details on the optical water type methodology are provided in the Lakes\_cci ATBD.

Several of the algorithms that may be considered for atmospheric correction are coupled atmosphere-water models yielding water-column properties including chlorophyll-a and suspended matter concentrations. These algorithms have not all been thoroughly evaluated in peer-reviewed literature and are included primarily for reference. Where they outperform better-understood alternatives they will be given further consideration.

The candidate algorithms are listed per sensor in the following tables. As a rule of thumb, only algorithms with a transparent and published methodology are considered. If they have been validated in a specific region, their validated range is given. The MERIS/OLCI algorithms (Table 3 and Table 4) are described in comparative detail in Neil et al. (2019). For the MODIS/VIIRS set of candidate algorithms (Table 5 for chlorophyll-a, Table 6 and Table 7 for suspended matter and turbidity) this comparison is still pending. Details on the wavebands combinations that are shown in these tables suggest there may be substantial overlap, in which case highly similar algorithms will be collapsed into algorithm types prior to calibration.

**Table 3 Candidate algorithms tested for MERIS (and OLCI by proxy) yielding chlorophyll-a concentration**

Type	Model	Reference
(Semi-)empirical NIR-red BR	MERIS 2-Band 708/665	Gilerson <i>et al.</i> 2010 Gurlin <i>et al.</i> 2011 Gons <i>et al.</i> 2005
	MERIS 2-Band 753/665	Gilerson <i>et al.</i> 2010 Gitelson <i>et al.</i> 2011 Moses <i>et al.</i> 2009.
	MERIS 3-Band	Gitelson <i>et al.</i> 2008 Gitelson <i>et al.</i> 2011 Gurlin <i>et al.</i> 2011 Moses <i>et al.</i> 2009
	MERIS NDCI	Mishra <i>et al.</i> 2012
Empirical OC	MERIS OC2E MERIS OC3E MERIS OC4E	O'Reilly <i>et al.</i> 2000

Type	Model	Reference
Neural Network	NN_Ch1 NN_IOP FUB CoastColour C2RLakes(EUT/BOR)	Ioannou <i>et al.</i> 2013
Analytical	MERIS QAA [Turbid]	Mishra <i>et al.</i> 2013
	MERIS GSM	Maritorena <i>et al.</i> 2002
	MERIS Matrix Inversion	Boss and Roesler 2006
Peak Height Method	MPH	Matthews <i>et al.</i> 2012

**Table 4 Candidate algorithms tested for MERIS (and OLCI by proxy) yielding total suspended matter.**

Type	Algorithm name	Reference
Empirical	Binding red Zhang 708 Vantrepotte 665 POWERS 560	Binding <i>et al.</i> 2005 Zhang <i>et al.</i> 2010 Vantrepotte <i>et al.</i> 2011 Eleveld <i>et al.</i> 2008
	D'Sa 665/560 Dekker 490,560 Dekker 560,665	D'Sa <i>et al.</i> 2007 Dekker <i>et al.</i> 2002
	Loisel 3-Band	Loisel <i>et al.</i> 2014
(Semi-) Analytical	Binding A Nechad 665 Nechad 681 Nechad 708 Nechad 753	Binding <i>et al.</i> 2010 Nechad <i>et al.</i> 2010

**Table 5 Summary of candidate Chla algorithms for MODIS/VIIRS**

Code	Name/form	Type	Bands*	Calibration or validated range	Reference
A	OC3M	blue-green band ratio	$\min[R_{rs}(443), R_{rs}(488)], R_{rs}(547)$	0.2 ~ 90 mg m <sup>-3</sup>	O'Reilly and Maritorena 2000
B	OC2M	blue-green band ratio	$R_{rs}(488), R_{rs}(547)$	0.2 ~ 90 mg m <sup>-3</sup>	O'Reilly and Maritorena 2000
C	OC2M-HI (500 m)	blue-green band ratio	$R_{rs}(469), R_{rs}(555)$	0.2 ~ 90 mg m <sup>-3</sup>	O'Reilly and Maritorena 2000

Code	Name/form	Type	Bands*	Calibration or validated range	Reference
D	FLH	peak height	$R_{rs}(665)$ , $R_{rs}(677)$ , $R_{rs}(746)$	1 – 10 mg m <sup>-3</sup>	Letelier 1996
E	linear	NIR-red band ratio	$R_{rs}(748)$ , [ $R_{rs}(667)$ or $R_{rs}(678)$ ]	4 – 240 mg m <sup>-3</sup>	Gitelson 1992; Dall’Olmo et al. 2005; Gitelson et al. 2007, 2008; Gurlin et al. 2011
F	linear	blue-green band ratio	$R_{rs}(551)$ , $R_{rs}(443)$	8 – 17 mg m <sup>-3</sup>	Ha et al. 2013
G	linear	spectral index	$R_{rc}(645)$ , $R_{rc}(859)$	6.6 – 113.7 mg m <sup>-3</sup>	Shi et al. 2017
H	APPEL model	empirical	$R(645)$ , $R(859)$ , $R(469)$	2.5 – 91.0 mg m <sup>-3</sup>	El-Alem et al. 2012
I	GSM	semi-analytical	(not reproduced)	0 – 100 mg m <sup>-3</sup>	Maritorena et al. 2002
J	QAA_v6	semi-analytical	(not reproduced)	0.02 – 70.21 mg m <sup>-3</sup>	Lee et al. 2002
K	QAA_Tur	semi-analytical	(not reproduced)	59 – 1376 mg m <sup>-3</sup>	Mishra et al. 2013, 2014
L	MODIS SA	semi-analytical	(not reproduced)	0 – 2 mg m <sup>-3</sup>	Carder et al. 2004

\*Reflectance bands are as used in the original definition, taking the following forms:

$R_{rs}$  is above-surface remote-sensing reflectance

$R_{rc}$  is the atmospherically Rayleigh-corrected reflectance.

**Table 6 Summary of candidate Turbidity algorithms for MODIS/VIIRS**

Code	Name/form	Type	Bands*	Calibration or validated range	Reference
A	polynomial	single red band	$R_{rs}(645)$	TSM <30 mg L <sup>-1</sup>	Petus et al. 2010
B	linear	single red band	$R_{rs}(645)$	Turb 0 – 15 NTU	Moreno-Madrinan et al. 2010
C	exponential	single red band	$R_{rs}(645)$	Turb 1.8 – 160 FTU	Constantin et al. 2017
D	power law	single red band	$R_{rs}(645)$	Turb 0.9 – 8 NTU	Chen et al. 2007
E	polynomial	single NIR band	$nL_w(869)$	Turb 1–300 NTU	Wang et al. 2012
F	power law	NIR-red ratio	$R_{rs}(859)/R_{rs}(645)$	Turb 50 – 1000 NTU	Robert et al. 2016
G	exponential	NIR-red ratio	$R(859)/R(645)$	Turb 77.4 – 2193 NTU TSM 77 – 2182 mg L <sup>-1</sup>	Doxaran et al. 2009
H	semi-empirical	red or NIR	$\rho_w(645)$ , $\rho_w(859)$	Turb 1.8 – 988 FNU	Dogliotti et al. 2015

\*Reflectance bands are as used in the original definition, taking the following forms:

$R_{rs}$  is above-surface remote-sensing reflectance

$nL_w$  is the normalized water-leaving radiance.

$R$  is the ‘surface reflectance’ of the MODIS land product.

$\rho_w$  is the water reflectance, which is defined as  $\pi L_w(\lambda) / E_d^+(\lambda)$ , where  $L_w$  is the water-leaving radiance and  $E_d^+$  is the above-water downwelling irradiance.

**Table 7 Summary of candidate TSM algorithms for MODIS/VIIRS**

Code	Name/form	Type	Bands*	Calibration or validated range	Reference
I	linear	single red band	$R(645)$	0 - 55 mg L <sup>-1</sup>	Miller and McKee 2004; Sipelgas et al. 2006
J	polynomial	single red band	$R_{rs}(645)$	0 - 30 mg L <sup>-1</sup>	Petus et al. 2010
K	exponential	single red band	$R_{rs}(645)$	0 - 300 mg L <sup>-1</sup>	Zhao et al. 2011; Shi et al. 2015
L	polynomial	single red band	$nL_w(645)$	0 - 16 mg L <sup>-1</sup>	Ondrusek et al. 2012
M	exponential	NIR-red ratio	$R(859)/R(645)$	77 - 2182 mg L <sup>-1</sup>	Doxaran et al. 2009
N	power law	NIR-red ratio	$R_{rs}(859)/R_{rs}(645)$	18 - 927 mg L <sup>-1</sup>	Robert et al. 2016
O	polynomial	NIR-red ratio	$\log[R_{rs}(859)]/\log[R_{rs}(645)]$	5.8 - 577.2 mg L <sup>-1</sup>	Chen et al. 2015
P	linear	NIR-red ratio	$\log[R_{rs}(859)]/\log[R_{rs}(645)]$	1 - 64 mg L <sup>-1</sup>	Wang et al. 2010a
Q	exponential	red and NIR	$R_t(645)-R_t(859)$	0 - 12 mg L <sup>-1</sup>	Hu et al. 2004
R	linear	red and NIR	$R_{rs}(645)-R_{rs}(859)$	0.3 - 20 mg L <sup>-1</sup>	Tarrant et al. 2010
S	linear	two NIR bands	$\rho_w(859)-\rho_w(1240)$	74 - 881 mg L <sup>-1</sup>	Wang et al. 2010b
T	exponential	three bands	$R_{rs}(488), R_{rs}(555), R_{rs}(645)$	1- 300 mg L <sup>-1</sup>	Zhang et al. 2010
U	semi-analytical	red	$nL_w(748)$	0.18 - 28.3 mg L <sup>-1</sup>	Binding et al. 2010
V	generic single-band	red or NIR	$\rho_w(645)$ or $\rho_w(859)$	1 -100 mg L <sup>-1</sup>	Nechad et al. 2010; Polito et al. 2016

\*Reflectance bands are as used in the original definition, taking the following forms:

$R$  is the ‘surface reflectance’ of the MODIS land product.

$R_{rs}$  is above-surface remote-sensing reflectance

$R_t$  is the total radiance observed by MODIS ( $F_t$ ) divided by the annual mean extraterrestrial solar irradiance  $F_0$ .

$nL_w$  is the normalized water-leaving radiance.

$\rho_w$  is the water reflectance, which is defined as  $\pi L_w(\lambda) / E_d^+(\lambda)$ , where  $L_w$  is the water-leaving radiance and  $E_d^+$  is the above-water downwelling irradiance.

## 6.2. Validation results for LWLR

Prior to the Lakes\_cci, extensive validation exercises were carried out of on satellite-derived LWLR against in situ remote-sensing reflectance (predominantly from above-water measurements) as well as on the retrieval of chlorophyll-a from atmospherically corrected LWLR. However, the number of satellite vs in situ matchups is limited and these analyses have mostly focussed on products derived from MERIS.

For LWLR, six algorithms for MERIS were initially compared: MEGS8.1 (MERIS default), FUB, CoastColour, Case2Regional, SCAPE-M and POLYMER. From these results (Figure 5 to Figure 7 give examples of MEGS and the best performing algorithms), POLYMER was selected based on its superior linearity and correlation with in situ data despite a significant negative bias, which appears to be associated with overestimation of the atmospheric radiance component rather than the water model, but this is not yet well understood. Linearity in the response nevertheless suggests that algorithms for the retrieval of chlorophyll-a, total suspended matter or turbidity can be tuned to reproduce in situ observations. This procedure is described in more detail in the E3UB document.

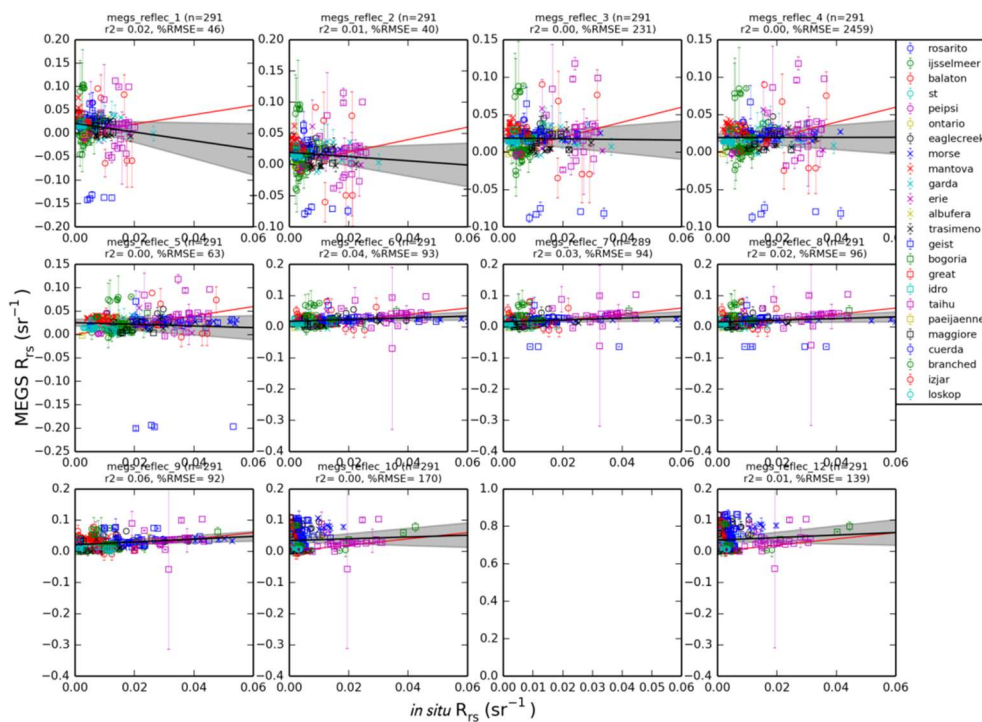


Figure 5 LWLR retrieval per MERIS waveband using the default MEGS algorithm. Matchups are for a  $\pm 7$ -day matchup window and 3x3 pixel extraction window and include results of 23 lakes.

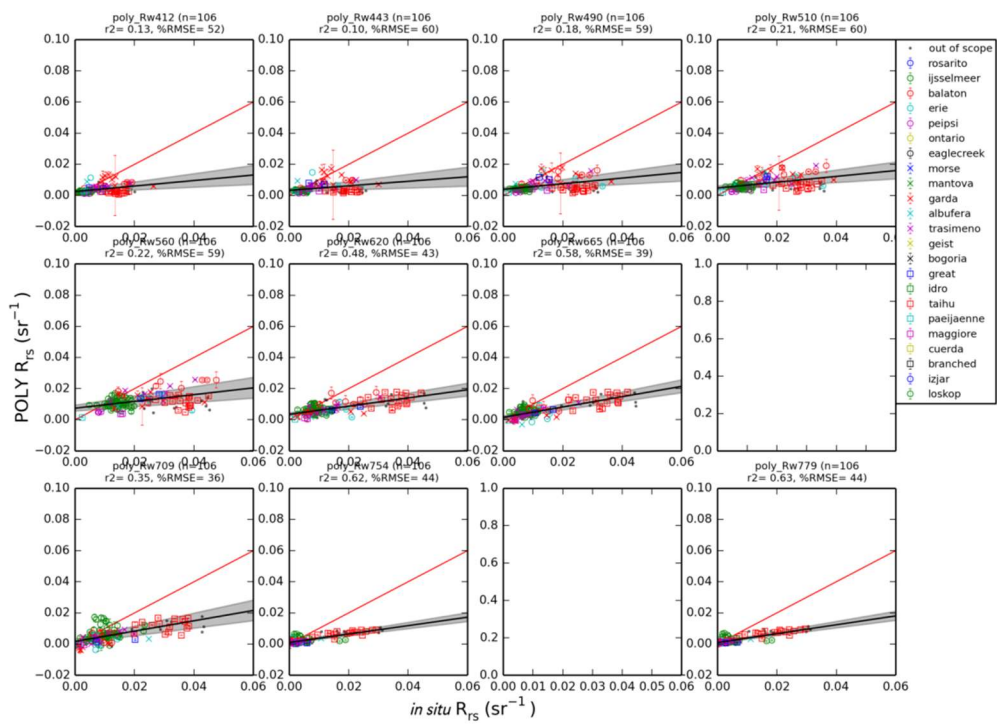


Figure 6 As previous but for the POLYMER algorithm.

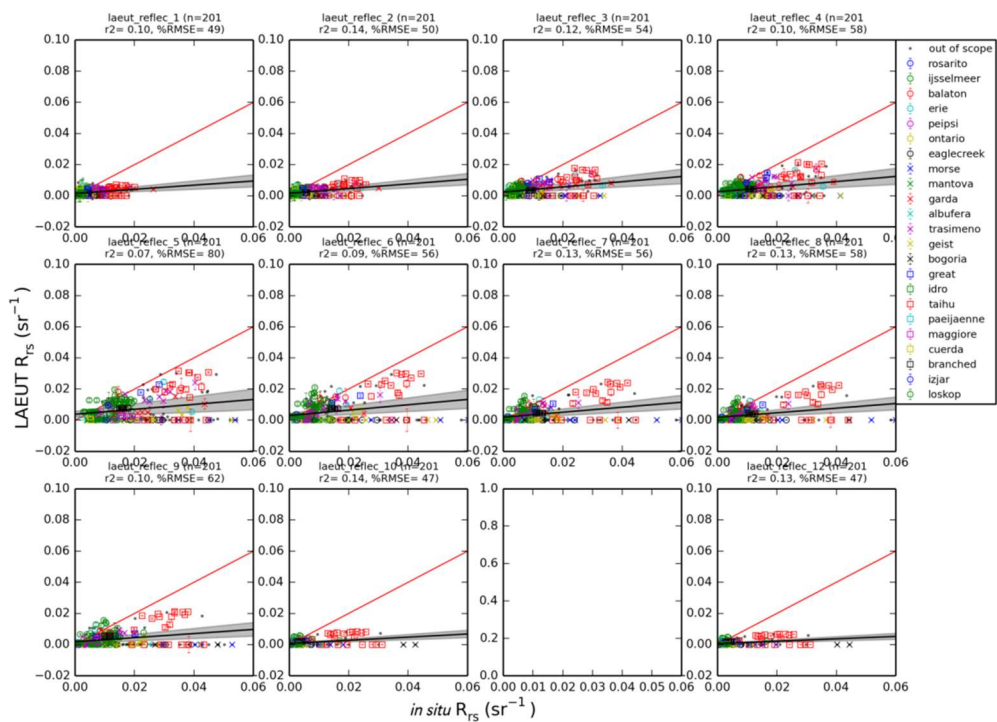
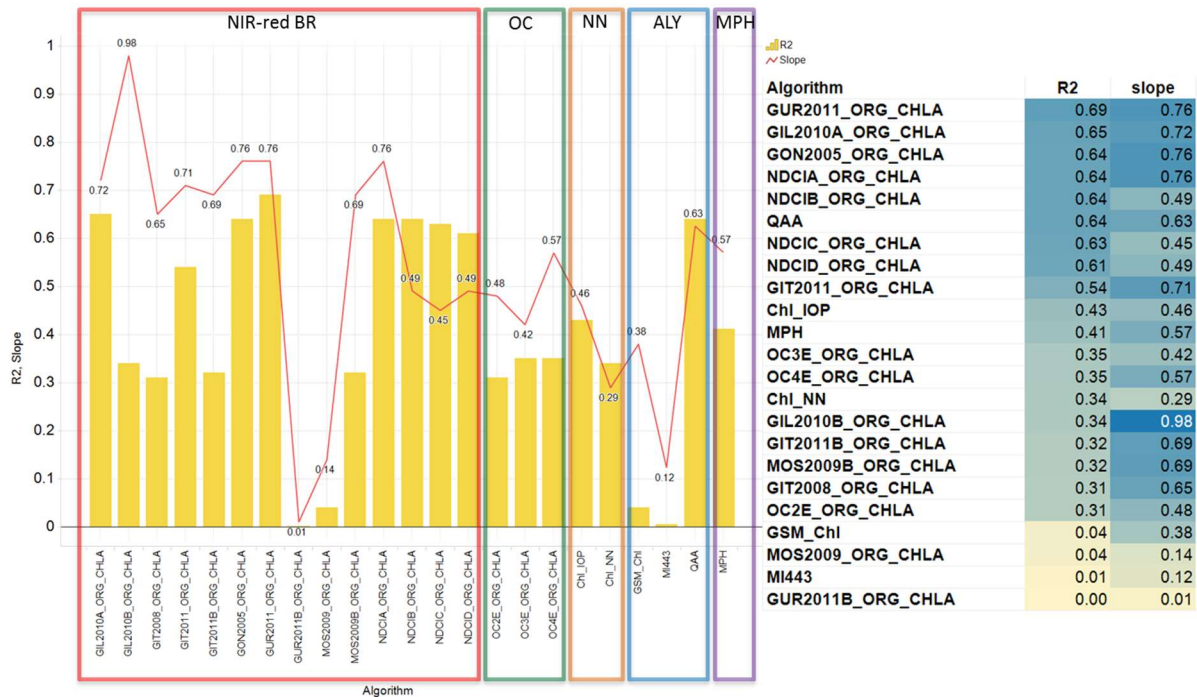


Figure 7 As previous but for the Lakes C2R algorithm.

Despite higher uncertainty in the validation of LWLR due to scarce in situ reference data, chlorophyll-a and suspended matter and/or turbidity algorithms may be evaluated and subsequently tuned based on a larger number of matchups with MERIS data in the LIMNADES data set for these measurands. Figure 8 shows results of the round-robin comparison of algorithms for chlorophyll-a,

ultimately resulting in the selection of OC2, a near infra-red (NIR) over red band algorithm based on Gilerson et al. (2010), the semi-analytical NIR-red ratio algorithm of Gons et al. (2005) and a modified Quasi-Analytical Algorithm (QAA) following Mishra et al. (2013). A separate algorithm tuning exercise was also carried out using exclusively in situ (reflectance and concentration) data, as reported by Neil et al. (2019).



**Figure 8 Round-robin comparison of chlorophyll-a retrieval algorithms, including NIR-red band ratio algorithms, ocean colour blue-green ratio algorithms, neural networks, analytical (multi-band) inversion algorithms and the maximum peak height algorithm.**

Algorithm comparisons for TSM and Turbidity have not yet been completed for the full set of candidate algorithms. An initial selection was made during GloboLakes based on the performance of TSM retrieval algorithms by Zhang et al. (2010), Binding et al. (2010) and Vantrepotte et al. (2011), which target different concentration ranges and optical water types. These algorithms were subsequently converted to Turbidity using the coefficients contained in the work by Nechad et al. (2010).

### 6.3. Identified issues for LWLR

For the retrieval of LWLR based on MERIS and OLCI using POLYMER there is a suspected systematic negative bias. The same bias observed in inland waters is not observed in coastal waters. Investigations are ongoing in collaboration with HYGEOS, the developers of POLYMER.

For chlorophyll-a retrieval from MODIS/VIIRS we note the following initial algorithm-specific issues:

- Algorithm D: the output of FLH requires an empirical calibration to convert to Chla.
- Algorithm G: this algorithm is developed in a turbid productive cyanobacteria-dominated lake. The MODIS-Aqua products used in this study are atmospherically Rayleigh-corrected. Further validation is needed.
- Algorithm H: the MODIS data used in this algorithm were corrected using the SMAC model (Simplified Method for Atmospheric Correction) which may not be suitable for a wide range of lakes or in near-shore waters.

- Algorithm J and K: the output of the two QAA-based models is phytoplankton absorption ( $a_{ph}$ ), the empirical relationship between  $a_{ph}$  and chlorophyll-a is subject to further research or tuning against in situ observations.

For Turbidity/TSM algorithms for MODIS/VIIRS:

- The wavebands at 645 nm and 859 nm are MODIS ‘land’ bands, which need to be produced alongside the standard ‘ocean’ bands for some of the algorithms to be implemented.
- For some extremely turbid waters, some specific atmospheric correction methods were employed:
  - Model E used the NIR-SWIR atmospheric correction algorithm developed by Wang and Shi (2007).
  - Algorithm K uses the atmospheric correction method based on dense vegetation targets developed by Guanter et al. (2007).
  - Algorithm U uses the iterative NIR correction of Stumpf et al. (2003).
  - Algorithm V used an atmospheric correction method by MUMM (Ruddick et al. 2000).

In all cases, existing validation results should be extended to the most current versions of atmospheric correction processors, observing calibration and validation data splits where the volume of satellite and in situ match-up data allows, noting where this is not the case. Details on this revised procedure are provided in the E3UB.

#### 6.4. Future improvements for LWLR validation

---

To address the issue of scarce in situ data, particularly outside the MERIS/MODIS period, we continue to engage with a variety of research groups and projects internationally. We also continue to seek sustained funding for LIMNADES and to bring in and screen data from national monitoring programmes. We are also involved in projects such as H2020 MONOCLE, which contributes to advancing the state of the art and lowering the cost of in situ radiometry to expand observation networks that directly support satellite validation in optically complex waters.

The OLCI instrument is configured with 12 more wavebands than SeaWiFS had. Many of these bands are intended to better capture variations in water colour or to separate the effects of water and atmosphere on the recorded radiance. We should, therefore, not expect the diagnostic retrieval of LWLR and derived water-column properties from SeaWiFS, MODIS and VIIRS to match that of MERIS and OLCI. Our research in Lakes\_cci is ultimately focussed on identifying and ultimately predicting the conditions under which retrieval from older sensors is of climate quality. This investigation will rely on geo-statistical approaches, climatologies and elements of optical modelling or water type classification. Unsuitable observation conditions may relate to e.g. atmospheric conditions, cloud cover and distance from land, but also specific lake conditions such as high wind-resuspension or exhibiting algal blooms. Simply removing such observation would likely introduce undesired bias into the data set - lakes that frequently fail to be reliably would then need to be removed. However, this would not skew the remaining observations towards conditions that can be consistently observed over long periods, which is equally undesirable. We will address this issue with climate modeller groups once sufficient evidence on long-term observation uncertainty has been collected.

#### 6.5. LWLR references

---

- Binding, C., Bowers, D., Mitchelson-Jacob, E. (2005). Estimating suspended sediment concentrations from ocean colour measurements in moderately turbid waters; the impact of variable particle scattering properties. *Rem Sens Env* 94(3): 373-383.
- Binding, C., Jerome, J., Bukata, R. and Booty, W. (2010). Suspended particulate matter in Lake Erie derived from MODIS aquatic colour imagery. *Int J Remote Sens* 31(19).
- Boss, E. and Roesler C. (2006). Over Constrained Linear Matrix Inversion with Statistical Selection. *In: Lee, ZP (Ed.), IOCCG Report nr 5. Remote Sensing of Inherent Optical Properties: Fundamentals, Tests of Algorithms, and Applications.*, pp. 126.

- Carder KL, Chen FR, Cannizzaro JP, et al (2004) Performance of the MODIS semi-analytical ocean color algorithm for chlorophyll-a. *Adv Space Res* 33:1152-1159.
- Chen S, Han L, Chen X, et al (2015) Estimating wide range Total Suspended Solids concentrations from MODIS 250-m imageries: An improved method. *ISPRS J Photogramm Remote Sens* 99:58-69.
- Chen Z, Hu C, Muller-Karger F (2007) Monitoring turbidity in Tampa Bay using MODIS/Aqua 250-m imagery. *Remote Sens Environ* 109:207-220.
- Constantin S, Constantinescu Ștefan, Doxaran D (2017) Long-term analysis of turbidity patterns in Danube Delta coastal area based on MODIS satellite data. *J Marine Syst* 170:10-21.
- Dall'Olmo G, Gitelson AA, Rundquist DC, et al (2005) Assessing the potential of SeaWiFS and MODIS for estimating chlorophyll concentration in turbid productive waters using red and near-infrared bands. *Remote Sens Environ* 96:176-187.
- Dekker, A. Vos, R., Peters, S. (2002). Analytical algorithms for lake water TSM estimation for retrospective analyses of TM and SPOT sensor data, *Int J Rem Sens* 23(1):15-35.
- Dogliotti AI, Ruddick KG, Nechad B, et al (2015) A single algorithm to retrieve turbidity from remotely-sensed data in all coastal and estuarine waters. *Remote Sens Environ* 156:157-168.
- Doxaran D, Froidefond J-M, Castaing P, Babin M (2009) Dynamics of the turbidity maximum zone in a macrotidal estuary (the Gironde, France): Observations from field and MODIS satellite data. *Estuar Coastal Shelf Sci* 81:321-332.
- El-Alem A, Chokmani K, Laurion I, El-Adlouni SE (2012) Comparative Analysis of Four Models to Estimate Chlorophyll-a Concentration in Case-2 Waters Using MODerate Resolution Imaging Spectroradiometer (MODIS) Imagery. *Remote Sens* 4:2373-2400.
- Eleveld, M., Pasterkamp, R., Van der Woerd, H., Pietrzak, J. (2008). Remotely sensed seasonality in the spatial distribution of sea-surface suspended particulate matter in the southern North Sea. *Est Coast Shelf Sci* 80(10): 103-113.
- Gitelson A (1992) The peak near 700 nm on radiance spectra of algae and water: relationships of its magnitude and position with chlorophyll concentration. *Int J Remote Sens* 13:3367-3373
- Gilerson, A., Gitelson, A., Zhou, J., Gurlin, D., Moses, W., Ioannou, I. and Ahmed, S. (2010). Algorithms for remote estimation of chlorophyll-a in coastal and inland waters using red and near infrared bands. *Opt Express* 18(23): 24109-24125.
- Gitelson, A., Dall'Olmo, G., Moses, W., Rundquist, D., Barrow, T., Fisher, T., Gurlin, D., Holz, J. (2008). A simple semi-analytical model for remote estimation of chlorophyll-a in turbid waters: Validation. *Remote Sens Environ* 112 (9), 3582-3593.
- Gitelson AA, Schalles JF, Hladik CM (2007) Remote chlorophyll-a retrieval in turbid, productive estuaries: Chesapeake Bay case study. *Remote Sens Environ* 109:464-472.
- Gitelson, A., Gurlin, D., Moses, W., Yacobi, Y. (2011). Remote estimation of Chlorophyll-a concentration in inland, estuarine, and coastal waters. *In: Weng, Q. (Ed.), Advances in Environmental Remote Sensing: Sensors, Algorithms, and Applications*. CRC Press, Taylor and Francis Group, pp. 449-478 (610 p. ISBN: 9781420091755).
- Gons H., Rijkeboer M., Ruddick K. (2005). Effect of a waveband shift on chlorophyll retrieval from MERIS imagery of inland and coastal waters. *J Plankton Res* 27(1):125-7.
- Guanter L, Del Carmen González-Sanpedro M, Moreno J (2007) A method for the atmospheric correction of ENVISAT/MERIS data over land targets. *Int J Remote Sens* 28:709-728
- Gurlin, D., Gitelson, A., Moses, W. (2011). Remote estimation of chl-a concentration in turbid productive waters – return to a simple two-band NIR-red model? *Remote Sens Environ* 115 (12), 3479-3490.
- Ha N, Koike K, Nhuan M (2013) Improved Accuracy of Chlorophyll-a Concentration Estimates from MODIS Imagery Using a Two-Band Ratio Algorithm and Geostatistics: As Applied to the Monitoring of Eutrophication Processes over Tien Yen Bay (Northern Vietnam). *Remote Sens* 6:421-442.
- Ioannou, I., Gilerson, A., Gross, B., Moshary, F., Ahmed, S. (2013). Deriving ocean color products using neural networks. *Remote Sens Environ* 134, 78e91.
- Lee Z, Carder KL, Arnone RA (2002) Deriving inherent optical properties from water color: a multiband quasi-analytical algorithm for optically deep waters. *Appl Opt* 41:5755-5772
- Letelier R (1996) An analysis of chlorophyll fluorescence algorithms for the moderate resolution imaging spectrometer (MODIS). *Remote Sens Environ* 58:215-223.
- Loisel, H., Mangin, A., Vantrepotte, V., Dessailly, D., Dinh, D.N., Garnesson, P. Ouillon, S., Lefebvre, J.P., Mériaux, X., Phan, T.M. (2014). Variability of suspended particulate matter

- concentration in coastal waters under the Mekong's influence from ocean color (MERIS) remote sensing over the last decade. *Rem Sens Environ* 150: 218-230.
- Maritorena, S., Siegel, D., Peterson, A. (2002). Optimization of a semianalytical ocean color model for global-scale applications. *Appl Opt* 41, 2705-2714.
- Miller RL, McKee BA (2004) Using MODIS Terra 250 m imagery to map concentrations of total suspended matter in coastal waters. *Remote Sens Environ* 93:259-266.
- Matthews, M., Bernard, S., Robertson, L. (2012). An algorithm for detecting trophic status (chlorophyll-a), cyanobacterial-dominance, surface scums and floating vegetation in inland and coastal waters. *Remote Sens Environ* 124, 637-652.
- Mishra, S., Mishra, D. (2012). Normalized difference chlorophyll index: a novel model for remote estimation of chlorophyll-a concentration in turbid productive waters. *Remote Sens Environ* 117, 394-406.
- Mishra S., Mishra D., Lee Z. (2014). Bio-optical inversion in highly turbid and cyanobacteria-dominated waters. (2014): *IEEE Trans Geosci Remote Sens* 52(1):375-88.
- Moreno-Madrinan MJ, Al-Hamdan MZ, Rickman DL, Muller-Karger FE (2010) Using the Surface Reflectance MODIS Terra Product to Estimate Turbidity in Tampa Bay, Florida. *Remote Sens* 2:2713-2728.
- Moses, W., Gitelson, A., Berdnikov, S., Povazhnyy, V. (2009). Satellite estimation of chlorophyll-a concentration using the red and NIR bands of MERIS – the Azov Sea case study. *IEEE Geosci Remote Sens Lett.* 6 (4), 845-849.
- Nechad, B., Dogliotti, A.I., Ruddick, K.G., Doxaran, D. (2016). Particulate Backscattering and suspended matter concentration retrieval from remote-sensed turbidity in various coastal and riverine turbid waters. *Proceedings of ESA Living Planet Symposium, Prague, 9-13 May 2016, ESA-SP 740.*
- Nechad, B., Ruddick, K., Park, Y. (2010). Calibration and validation of a generic multisensor algorithm for mapping of total suspended matter in turbid waters". *Remote Sens Environ* 114 (2010) 854-866.
- Neil, C., Spyarakos, E., Hunter, P., Tyler, A. (2019). A global approach for chlorophyll-a retrieval across optically complex inland waters based on optical water types. *Remote Sens Environ* 229: 159-178.
- Ondrusek M, Stengel E, Kinkade CS, et al (2012) The development of a new optical total suspended matter algorithm for the Chesapeake Bay. *Remote Sens Environ* 119:243-254.
- O'Reilly, J, Maritorena, S., O'brien, M., Siegel, D., Toole, D., Menzies, D., Smith, R. et al. (2000). SeaWiFS postlaunch calibration and validation analyses, part 3. NASA tech. memo 206892, no. 11 (2000): 3-8.
- Petus C, Chust G, Gohin F, et al (2010) Estimating turbidity and total suspended matter in the Adour River plume (South Bay of Biscay) using MODIS 250-m imagery. *Cont Shelf Res* 30:379-392.
- Polito CD, Di Polito C, Ciancia E, et al (2016) On the Potential of Robust Satellite Techniques Approach for SPM Monitoring in Coastal Waters: Implementation and Application over the Basilicata Ionian Coastal Waters Using MODIS-Aqua. *Remote Sens* 8:922.
- Robert E, Grippa M, Kergoat L, et al (2016) Monitoring water turbidity and surface suspended sediment concentration of the Bagre Reservoir (Burkina Faso) using MODIS and field reflectance data. *Int J Appl Earth Obs.* 52:243-251.
- Ruddick KG, Ovidio F, Rijkeboer M (2000) Atmospheric correction of SeaWiFS imagery for turbid coastal and inland waters. *Appl Opt* 39:897-912.
- D'Sa, E. , Miller, R., McKee, B. (2007). Suspended particulate matter dynamics in coastal waters from ocean color: Application to the northern Gulf of Mexico, *Geophys Res Lett* 34, L23611.
- Spyrakos E, O'Donnell R, Hunter PD, Miller C, Scott M, Simis S, et al. (2018). Optical types of inland and coastal waters. *Limnol Oceanogr.* 63(2).
- Stumpf, R.P., A Rnone, R.A., Gould, R.W., Martinolich, P.M. and R Ansibrahmanakul, V., 2003, A partially coupled ocean-atmosphere model for retrieval of water-leaving radiance from SeaWiFS in coastal waters. In *SeaWiFS Postlaunch Technical Report Lake Erie SPM derived from MODIS imagery Series, Volume 22: Algorithm Updates for the Fourth SeaWiFS Data Reprocessing.* NASA Technical Memorandum 2003-206892.
- Shi K, Zhang Y, Zhou Y, et al (2017) Long-term MODIS observations of cyanobacterial dynamics in Lake Taihu: Responses to nutrient enrichment and meteorological factors. *Sci Rep* 7:40326.
- Shi K, Zhang Y, Zhu G, et al (2015) Long-term remote monitoring of total suspended matter concentration in Lake Taihu using 250m MODIS-Aqua data. *Remote Sens Environ* 164:43-56.

- Sipelgas L, Raudsepp U, Kõuts T (2006) Operational monitoring of suspended matter distribution using MODIS images and numerical modelling. *Adv Space Res* 38:2182-2188.
- Tarrant PE, Amacher JA, Neuer S (2010) Assessing the potential of Medium-Resolution Imaging Spectrometer (MERIS) and Moderate-Resolution Imaging Spectroradiometer (MODIS) data for monitoring total suspended matter in small and intermediate sized lakes and reservoirs. *Water Resour Res* 46.
- Vantrepotte, V., Loisel, H., Mériaux, X. Neukermans, G. Dessailly, D. Jamet, C., Gensac, E., Gardel, A. (2011). Seasonal and inter-annual (2002-2010) variability of the suspended particulate matter as retrieved from satellite ocean color sensor over the French Guiana coastal waters. *J Coast Res SI* 64 (Proceedings of the 11th International Coastal Symposium).
- Wang H, Hladik CM, Huang W, et al (2010a) Detecting the spatial and temporal variability of chlorophyll-a concentration and total suspended solids in Apalachicola Bay, Florida using MODIS imagery. *Int J Remote Sens* 31:439-453.
- Wang J-J, Lu XX, Liew SC, Zhou Y (2010b) Remote sensing of suspended sediment concentrations of large rivers using multi-temporal MODIS images: an example in the Middle and Lower Yangtze River, China. *Int J Remote Sens* 31:1103-1111.
- Wang M, Nim CJ, Son S, Shi W (2012) Characterization of turbidity in Florida's Lake Okeechobee and Caloosahatchee and St. Lucie Estuaries using MODIS-Aqua measurements. *Water Res* 46:5410-5422.
- Wang M, Shi W (2007) The NIR-SWIR combined atmospheric correction approach for MODIS ocean color data processing. *Opt Express* 15:15722-15733.
- Zhang, Y., Shi, K., Liu, X., Zhou, Y., Qin., B. (2014). Lake topography and wind waves determining seasonal-spatial dynamics of total suspended matter in turbid lake Taihu, China: assessment using long-term high-resolution MERIS data. *PLoS ONE* 9(5): e98055.
- Zhao H, Chen Q, Walker ND, et al (2011) A study of sediment transport in a shallow estuary using MODIS imagery and particle tracking simulation. *Int J Remote Sens* 32:6653-6671.

## 7. Conclusions

In summary, the main issues observed in the state-of-the-art methodologies used to produce CRDP V1, and therefore focussing our activities towards CRDP V2, are as follows.

For **Lake Water Level (LWL)**, the algorithm has been developed at LEGOS since several years and the theoretical basis is well understood. It has been largely validated and applied over a large number of studies. The limitations are however not negligible and need further improvements over the next two years. The most notable expected improvement is a dedicated DEM uploaded to current ESA missions, to better the small lakes particularly in regions with surrounding relief, like mountain areas. New reprocessing of past missions, with the current retracking algorithms will also be performed in order to provide longer and more accurate time series for small lakes. And finally, we are implementing new methods for SAR processing on sentinel-3A and sentinel-3B satellite known as full SAR processing, which will allow sub meter resolutions along the track of the satellite.

The lake water extent (**LWE**) variable is generated using Optical and SAR imagery. Optical methodologies exploit the low reflectance characteristic of water bodies in the SWIR spectral domain, and also in the NIR domain applying either classification approaches or thresholding ones. The optical approaches are very sensitive to cloud cover (even at local scale) but also to environmental conditions. SAR methodologies exploit the low backscatter presented by lake waters applying classification techniques and spatial contrast operators. Water surface variability (wind, ice, vegetation, shallow water) drives the SAR product accuracy. LWE is jointly used with LWL to derive hypsometric curves that can also be considered as a source of indirect LWE validation. The joint exploitation of both Optical and SAR products remains a promising issue that will be considered, but visual validation remains a critical component.

The **lake ice cover (LIC)** product is generated from a threshold-based algorithm using MODIS surface reflectance data (MOD09/MYD09). Validation results indicate that classification errors are expected to be within ca. 1 to 8 % depending on class (ice cover, open water, cloud cover) for the LIC variable contained in CRDP V1. A few issues have been identified with the LIC product that merit further work leading to the release of CRDP V2, including assessment of the impact of thin clouds and large solar zenith angles on retrieval performance, water detection as to avoid false positives (ice detection when lakebeds are dry), as well as full characterization and quantification of uncertainty beyond the classification errors currently reported. Ongoing and future activities will also examine the potential of machine learning classifiers applied to TOA reflectance data from MODIS, VIIRS and Sentinel-3 for Lakes\_cci LIC V2 algorithm.

For **Lake Surface Water Temperature (LSWT) v5.0 (Lake CCI v2)**, the following can be foreseen. The issue of error covariance estimation for optimal estimation is a long-standing problem, to which a possible solution (Merchant et al., 2019) has recently been proposed. These techniques will be applied within SST CCI and the matrices will be applicable for LSWT v5.0. MODIS will be added to the processed data stream, either on the same algorithmic basis as Metop AVHRRs, or with additional improvements using MODIS capabilities if research yields these in time (particularly, exploitation of the 8.7 um channel). LSWT v5.0 will have switched from ERA-interim to ERA-5 for background numerical weather prediction information.

The **Lake Water Leaving Reflectance (LWLR)** algorithm chain, despite known issues with separation of atmospheric and water-leaving radiance, is known to produce biogeochemical and physical estimates of chlorophyll-a and turbidity which outperform individually published algorithms, due to the use of an adaptive algorithm chain based in *a priori* Optical Water Type classification. The major challenge towards producing a truly long-term CDR is the adoption of legacy sensors which lack wavebands which are essential in providing the current level of accuracy. The procedures described in the E3UB to provide per-pixel uncertainty estimates will be pivotal in selecting geographic areas where inter-sensor responses can be reliable compared.

Overall, and to no surprise, the use of a wide range of observation principles to address the Lakes ECVs has led to a degree of parallel evolution in classification methods for land, water, cloud and ice detection that underpin most of our approaches. Whether each approach classifies the same number of water pixels is not of utmost importance - it is the confidence in the retrieved quantities

that matters far more. However, systematic differences in the water pixel classification will have to be evaluated using the results produced for the first version of the Lakes climate data record.

Five use cases will start once V1 of the Lakes CDR is completed. These are equally important in determining whether the quality of the thematic ECVs is sufficient to determine consistent trends between observed variables, within the context of existing knowledge of the study areas.